Whispering-gallery-mode microdisk lasers produced by femtosecond laser direct writing

Jin-Feng Ku,[1] Qi-Dai Chen,[1,3] Ran Zhang,[1] and Hong-Bo Sun[1,2,4]

[1]*State Key Laboratory on Integrated Optoelectronics, College of Electronic Science and Engineering, Jilin University, 2699 Qianjin Street, Changchun 130012, China*

[2]*College of Physics, Jilin University, 119 Jiefang Road, Changchun 130023, China*

[3]*e-mail: chenqd@jlu.edu.cn*

[4]*e-mail: hbsun@jlu.edu.cn*

We report in this Letter fabrication of whispering-gallery-mode microdisk lasers by femtosecond laser direct writing of dye-doped resins. Not only is well-defined disk shape upheld on an inverted cone-shaped supporter, but the disk also exhibits significant lasing actions characteristic of an abrupt increase of light output and the significant narrowing of the spectral lines when the threshold is approached. This work shows that the laser micronanofabrication technology is not only applicable to passive micro-optical components, but also it may play an important role in fabrication of active optoelectronic devices and their integrated photonic circuits.   © 2011 Optical Society of America

OCIS codes: 140.3410, 140.3945, 250.2080.

Since being introduced in three-dimensional (3D) fabrication, femtosecond laser direct writing (FsLDW) via two-photon induced photopolymerization [1–10] has been widely utilized in producing various micro-optical [3,4], microelectronic [5,6], micromechanical [7,8], microfluidic [9,10], and many other microdevices and systems [11]. Its role has been established due to its intrinsic 3D prototyping capability with nanometric spatial resolution [1,2,11]. Particularly, the high prototyping accuracy and the surface roughness at the order of a few nanometers are the two key factors that guarantee the optical quality of microdevices. Among many convincing proofs, Gong's group [12] reports recently on high-Q polymer whispering-gallery microcavities written by two-photon photopolymerization of zirconium/silicon hybrid sol-gel. Such devices may find broad uses in cavity quantum electrodynamics, ultrasmall optical filters, low threshold lasers, and biosensors [13]. Compared with the passive components, active devices, such as lasers, are equally important for integrated photonic circuits as lasers. Microlasers based on whispering-gallery-mode (WGM) typically fall into three regimes [14], microspheres, microrings, and microdisks, and have been studied extensively since the early demonstration by Garrett *et al.* [15]. The designability of the geometrical shapes and fine surface structures of the cavities remain technically challenging due to the limitation of each technology, e.g., droplets formation [16], lithography [17], and use of colloidal spheres [18]. Also, devices have to be produced separately and mounting them in an integrated photonic circuit imposes additional difficulties for practical use. If the delicate FsLDW approach could be applied, not only could artificially designed 3D shapes and structures be realized, but the microcavity lasers may be designed and *in situ* created. The lasers can be integrated with other devices produced by the same means into an entire photonic integrated system." This may pave a new avenue towards deep insight cavity electrodynamics and realization of new concept photonic integrated circuits.

As the first step to reach the above end, we report in this Letter realization of microdisk lasers by FsLDW via two-photon photopolymerization of Rhodamine B (RhB) doped epoxy-based negative resin SU-8. Not only is well-defined suspended disk shape created, but it also demonstrates significant lasing action under a picosecond laser pumping.

Shown in Figs. 1(a) and 1(b) are the optical microscopic images of the WGM microdisk lasers. For FsLDW, a Ti:Sapphire femtosecond laser (Tsunami, Spectra-Physics) operating at 120 fs pulse width, central wavelength of 790 nm, and mode locked at a repetition rate of 80 MHz was employed. The laser beam was tightly
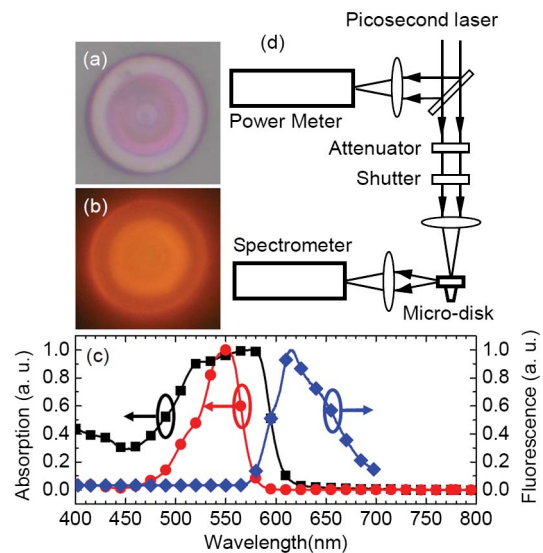

Fig. 1.   (Color online) Microdisk laser created by femtosecond laser direct writing (FsLDW) via two-photon-induced photopolymerization. Optical microscopic images of the disk under top illumination (a) by weak white-light and (b) by relatively strong blue-light excitation. (c) Absorption spectra of the RhB (circle), RhB-doped SU-8 (square), and the photoluminescence spectrum of the mixed resin (diamond). (d) Picosecond pumping and signal analysis system.

focused by a high numerical aperture (NA = 1.35,100×) oil immersion objective lens. The laser beam measured before the objective lens was only 8 mw. The focal spot was scanned laterally by a two-galvano-mirror set, and was moved along the optical axis by a piezoelectric stage. All the 3D motions have accuracy around 1 nm. The functional material was RhB-doped SU-8 with an overall concentration of 1 wt%. The chosen concentration of 1 wt% is a trade-off between lasing action and fabrication process. In fact, concentrations between 1 wt% and 2 wt% are satisfying. The mixed resin was prepared by spincoating on microscopic cover slides that were cleaned with acetone, absolute ethanol, and deionized water. After a soft-bake step for 50 minutes at 95 °C to evaporate the solvents, thick films were obtained. During FsLDW according to preprogrammed patterns [1–10], acid was generated with a concentration following the distribution of the square of the light intensity. Then, the patterned photoresists were post-baked at a temperature of 95 °C for 15 minutes, whereby the latent images were converted into cross-linked solid skeleton by a cationic photoamplificaton. Finally, the sample was developed in acetone for 60 seconds to remove the unsolidified resin.

The absorption peaks of RhB and RhB-doped SU-8 are both centered at around 550 nm and the red edges extend to not longer than 620 nm. The linear absorption at 790 nm of the doped resin is negligible and the fluorescence peaks at 615 nm. Under optical microscope, the outer portion of the disk exhibits light pink color while the relatively deeper color rings [Fig. 1(a)] in the middle are a reflection of the projective superimposition of the disk and the supporting wall beneath. Excited by blue light from a mercury lamp, the structure shows a strong orange color [Fig. 1(b)]. The disk structure is thus revealed here and in details by the scanning electron microscopic (SEM) images. Figure 2(a) is the top view and (b) the tilted view of the WGM microdisk. It consists of two parts, the inverted cone-shaped supporter and the disk with a slightly slanted edge, which is expected for better optical mode concentration. The diameters of the disk, the upper and lower ends of the cone, are 20 μm, 14 μm,

and 8 μm, respectively. The supporter is internally empty with a wall of 3 μm thickness.

When the structure is universally pumped from the top [Fig. 1(d)], photons emitted from the periphery of the disk, undergoing mode selection, form WGMs and are not disturbed by the central pedestal portion. For optical pumping, a picosecond laser of wavelength 532 nm (frequency doubled from a 1064 nm laser), pulsewidth of 15 ps, and a repetition rate of 50 KHz was chosen. The laser beam is focused with a $f = 160$ mm long working distance lens from the disk top. The light intensity is adjusted by an attenuator and a shutter was used to control the pumping interval. The light cycled inside the WGM modes is slightly scattered from the side edge due to the surface roughness [the inset of Fig. 2(b)], which is collected from the side by a CCD (charge coupled devices)-equipped spectrometer [Fig. 1(d)]. Experimentally, it is found that the increase of the pumping light intensity (I) led to an abrupt rise of the laser output at $I_{th} = 634$ mW/cm^2. The highest peak at the wavelength around 639 nm is the result of mode competition. The existence of the significant threshold is a fingerprint of the lasing action [Fig. 3(a)]. The linear increase of the laser intensity versus pump lasts till ~$3I_{th}$, where the output becomes saturated [The top inset of Fig. 3(a)]. When the pump power intensity exceeds three I_{th}, the output decreases slowly. This is a combination of gain saturation and effect of dye photobleaching.

In order to form a stable oscillation in the cavity and make light waves strengthened due to interference, the phase change for the light going a roundtrip in the cavity should be an integer multiple of 2π, i.e., the resonance condition:

$$2\pi n r = m\lambda, \tag{1}$$

where n and r are the refractive index and radius of the disk, respectively, and m is an integer. Restricted by the condition, only certain frequencies of light are ultimately
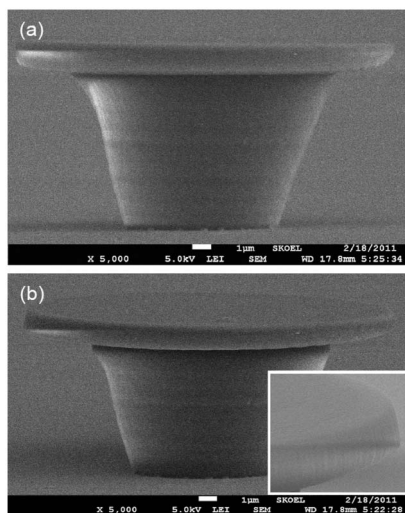

Fig. 2.   SEM images of the WGM microdisk laser. (a) Side of the microdisk system, and (b) tilted view. Inset magnification shows the surface roughness of the disk's edge.
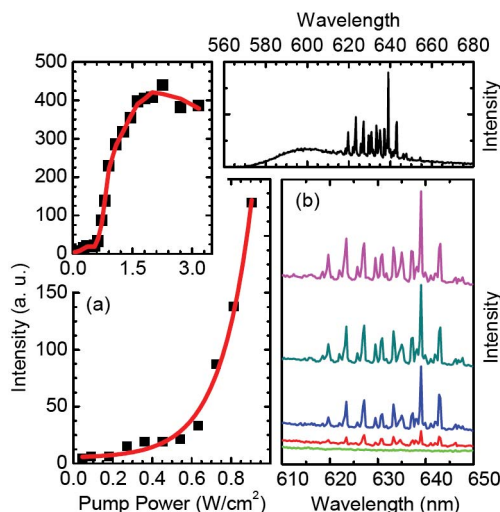

Fig. 3.   (Color online) Lasing of the WGM microdisk lasers. (a) Light output versus pumping laser intensity, and the top inset gives expanded wavelength range dependence. (b) Emission spectra of the microdisk laser at varied pumping intensity, i.e., 0.6, 1.1, 1.7, 2.3, 2.9 I_{th}. Slow protrusion in the top inset should come from the inverted cone supporter.
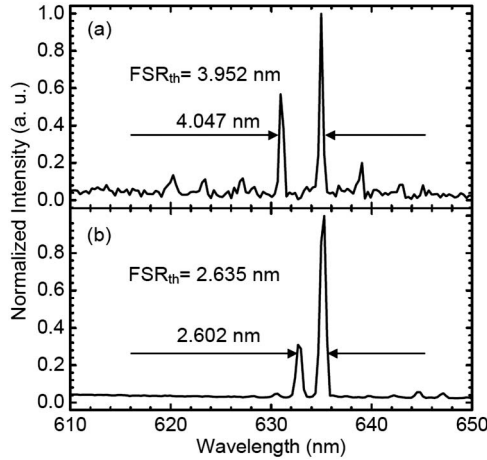
Fig. 4. Disk-diameter dependent lasing spectra with measured and theoretical FSR from (a) disk with $d = 20\,\mu$m and (b) disk with $d = 30\,\mu$m.

chosen and are enhanced by the cavity. The frequency range is discerned from the simultaneously recorded spectra of the scattering from the WGM disk [Fig. 3(b)]. By derivation of both sides of Eq. (1), we have

$$\Delta\lambda = \lambda^2 / 2\pi n r, \qquad (2)$$

where $\Delta\lambda$ is free spectral range (FSR). Judging from Eq. (2), one finds $\Delta\lambda$ is inversely proportional to the radius of the disk for a given material at an identical wavelength. For $d = 20\,\mu$m, the measured FSR = 4.047 nm, agreeing well with the theoretically predicted value about 3.952 nm [Fig. 4(a)].

Quality factor (Q) is a typical factor used to evaluate the capability that a cavity stores energy, which is defined as 2π times the number of optical cycles required for the cavity mode field to decay to $1/e$ of its initial value. For an isolated microdisk, Q is determined by [19–21]

$$Q^{-1} = Q_{\text{abs}}^{-1} + Q_{\text{scat}}^{-1} + Q_{\text{cav}}^{-1}. \qquad (3)$$

The inverse of Q_{abs}, Q_{scat}, and Q_{cav} corresponds to absorption loss, scattering loss, and cavity finesse, respectively. In the above equation, the second term Q_{scat}^{-1} is a key role for the Q value of the microdisk laser in the current study, while the first item Q_{abs}^{-1} is less important because both SU8 and Rhodamin are transparent in the visible wave range; also the Q_{cav}^{-1} is small relative to Q_{scat}^{-1}. So, the total Q factor of the WGM microdisk is sensitively affected by its surface roughness and shape deformation, which are feasibly controllable in the process of laser fabrication. The Q factor of WGM can be roughly calculated according to the spectral parameters:

$$Q = \lambda / \delta\lambda, \qquad (4)$$

where λ is the resonance wavelength and $\delta\lambda$ is the full width at half-maximum (FWHM). For the disk shown in Fig. 2 ($d = 20\,\mu$m), Q was calculated to be 1654 in the lasing region [Fig. 4(a)], and $Q = 930$ for the disk with $d = 30\,\mu$m, [Fig. 4(b)]. Both are not satisfying, still

far from the best results achieved from WGM structures produced by other means, at the level 10^6 order and even greater. [13] However, the low Q value and the relatively large threshold of lasing are not intrinsic to the fabrication technology itself since much better defined structures have been achieved. Improving the performance of the laser devices is an immediate task of our future study.

In summary, we report in this Letter lasing actions of a WGM microdisk laser created by a FsLDW approach. This should be an important step for the delicate micro-nanofabrication technology entering from the micro-optics to the optoelectronic fields and it may open a new avenue towards integrated photonic circuits.

References

1. S. Maruo, O. Nakamura, and S. Kawata, Opt. Lett. **22**, 132 (1997).
2. S. Kawata, H. B. Sun, T. Tanaka, and K. Takada, Nature **412**, 697 (2001).
3. M. P. Joshi, H. E. Pudavar, J. Swiatkiewicz, P. N. Prasad, and B. A. Reianhardt, Appl. Phys. Lett. **74**, 170 (1999).
4. D. Wu, Q. D. Chen, L. G. Niu, J. Jiao, H. Xia, J. F. Song, and H. B. Sun, IEEE Photon. Technol. Lett. **21**, 1535 (2009).
5. Y. L. Zhang, L. Guo, S. W. Wei, Y. Y. He, H. Xia, Q. D. Chen, H. B. Sun, and F. S. Xiao, Nano Today **5**, 15 (2010).
6. B. B. Xu, H. Xia, L. G. Niu, Y. L. Zhang, K. Sun, Q. D. Chen, Y. Xu, Z. Q. Lv, Z. H. Li, H. Misawa, and H. B. Sun, Small **6**, 1762 (2010).
7. S. Maruo and H. Inoue, Appl. Phys. Lett. **91**, 084101 (2007).
8. H. Xia, J. Wang, Y. Tian, Q. D. Chen, X. B. Du, Y. L. Zhang, Y. He, and H. B. Sun, Adv. Mater. **22**, 3204 (2010).
9. F. He, H. Xu, Y. Cheng, J. L. Ni, H. Xiong, Z. Z. Xu, K. Sugioka, and K. Midorikawa, Opt. Lett. **35**, 1106 (2010).
10. J. Wang, Y. He, H. Xia, L. G. Niu, R. Zhang, Q. D. Chen, Y. L. Zhang, Y. F. Li, S. J. Zeng, J. H. Qin, B. C. Lin, and H. B. Sun, Lab Chip **10**, 1993 (2010).
11. Y. L. Zhang, Q. D. Chen, H. Xia, and H. B. Sun, Nano Today **5**, 435 (2010).
12. Z. P. Liu, Y. Li, Y. F. Xiao, B. B. Li, X. F. Jiang, Y. Qin, X. B. Feng, H. Yang, and Q. H. Gong, Appl. Phys. Lett. **97**, 211105 (2010).
13. F. Vollmer and S. Arnold, Nat. Methods **5**, 591 (2008).
14. X. D. Fan, I. M. White, S. I. Shopova, H. Y. Zhu, J. D. Suter, and Y. Z. Sun, Anal. Chim. Acta **620**, 8 (2008).
15. C. G. B. Garrett, W. Kaiser, and W. L. Bond, Phys. Rev. **124**, 1807 (1961).
16. S. K. Y. Tang, Z. Y. Li, A. R. Abate, J. J. Agresti, D. A. Weitz, D. Psaltis, and G. M. Whitesides, Lab Chip **9**, 2767 (2009).
17. Y. H. Yang, Y. Zhang, N. W. Wang, C. X. Wang, B. J. Li, and G. W. Yang, Nano Scale **3**, 592 (2011).
18. T. Mitsui, Y. Wakayama, T. Onodera, Y. Takaya, and H. Oikawa, Nano Lett. **8**, 853 (2008).
19. S. Arnold and S. I. Shopova, in *Biophotonics: Spectroscopy, Imaging, Sensing, and Manipulation (NATO Science for Peace and Security Series B: Physics and Biophysics)* 1st ed. (Springer, Netherlands, 2010).
20. M. Kuwata-Gonokami and K. Takeda, Opt. Mater. (Amsterdam) **9**, 12 (1998).
21. F. Sasaki, S. Kobayashi, S. Haraichi, S. Fujiwara, K. Bando, Y. Masumoto, and S. Hotta, Adv. Mater. **19**, 3653 (2007).